Обзор ArXiv:astro-ph, 5-10 июня 2016

От Сильченко О.К.

Astro-ph: 1606.00867

SURFACE BRIGHTNESS PROFILES OF DWARF GALAXIES: II. COLOR TRENDS AND MASS PROFILES

Kimberly A. Herrmann[1], Deidre A. Hunter[2], & Bruce G. Elmegreen[3]
[1]Penn State Mont Alto, 1 Campus Drive, Mont Alto, PA 17237, USA; kah259@psu.edu
[2]Lowell Observatory, 1400 West Mars Hill Road, Flagstaff, AZ 86001, USA; dah@lowell.edu and
[3]IBM T. J. Watson Research Center, 1101 Kitchawan Road, Yorktown Hts., NY 10598, USA; bge@us.ibm.com

ABSTRACT

In this second paper of a series, we explore the $B-V$, $U-B$, and FUV−NUV radial color trends from a multi-wavelength sample of 141 dwarf disk galaxies. Like spirals, dwarf galaxies have three types of radial surface brightness profiles: (I) single exponential throughout the observed extent (the minority), (II) down-bending (the majority), and (III) up-bending. We find that colors of (1) Type I dwarfs generally become redder with increasing radius unlike spirals that have a blueing trend that flattens beyond ∼1.5 disk scale lengths, (2) Type II dwarfs come in six different "flavors," one of which mimics the "U" shape of spirals, and (3) Type III dwarfs have a stretched "S" shape where central colors are flattish, become steeply redder to the surface brightness break, then remain roughly constant beyond, similar to spiral Type III color profiles, but without the central outward bluing. Faint ($-9 > M_B > -14$) Type II dwarfs tend to have continuously red or "U" shaped colors and steeper color slopes than bright ($-14 > M_B > -19$) Type II dwarfs, which additionally have colors that become bluer or remain constant with increasing radius. Sm dwarfs and BCDs tend to have at least some blue and red radial color trend, respectively. Additionally, we determine stellar surface mass density (Σ) profiles and use them to show that the break in Σ generally *remains* in Type II dwarfs (unlike Type II spirals) but generally *disappears* in Type III dwarfs (unlike Type III spirals). Moreover, the break in Σ is strong, intermediate, and weak in faint dwarfs, bright dwarfs, and spirals, respectively, indicating that Σ may straighten with increasing galaxy mass. Lastly, the average stellar surface mass density at the surface brightness break is roughly 1−2 $M_\odot$ pc^{-2} for Type II dwarfs but higher at 5.9 $M_\odot$ pc^{-2} or 27 $M_\odot$ pc^{-2} for Type III BCDs and dIms, respectively.

Subject headings: galaxies: dwarf — galaxies: fundamental parameters — galaxies: irregular — galax

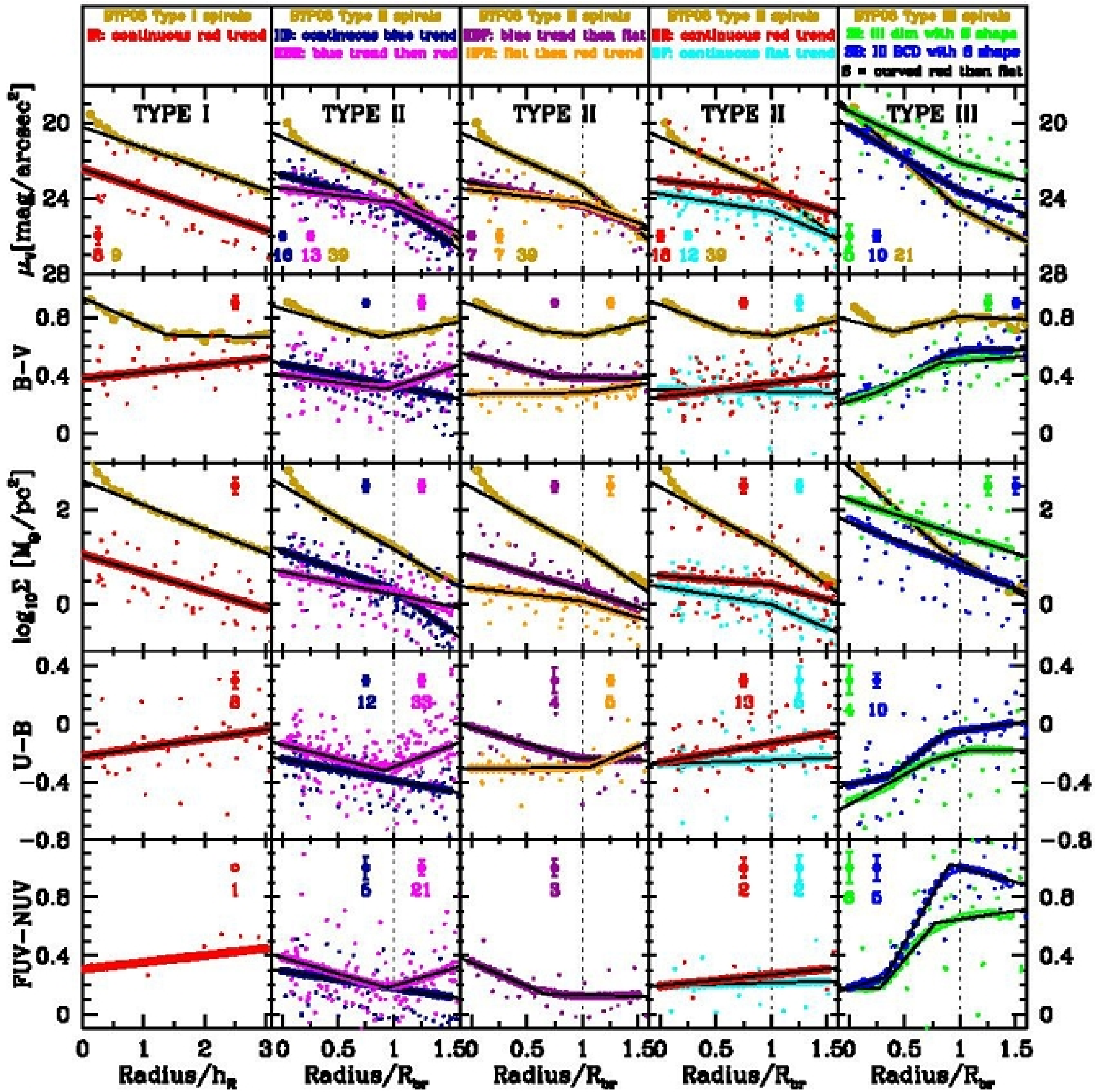

1.— Scaled and averaged profiles for the *broken-by-default* sample (broken-by-default means that galaxies which had profile
e interpreted as either one component or two components were given two components in this sample): *Top row*: V-band

То же самое, с разбивкой типа II по светимости

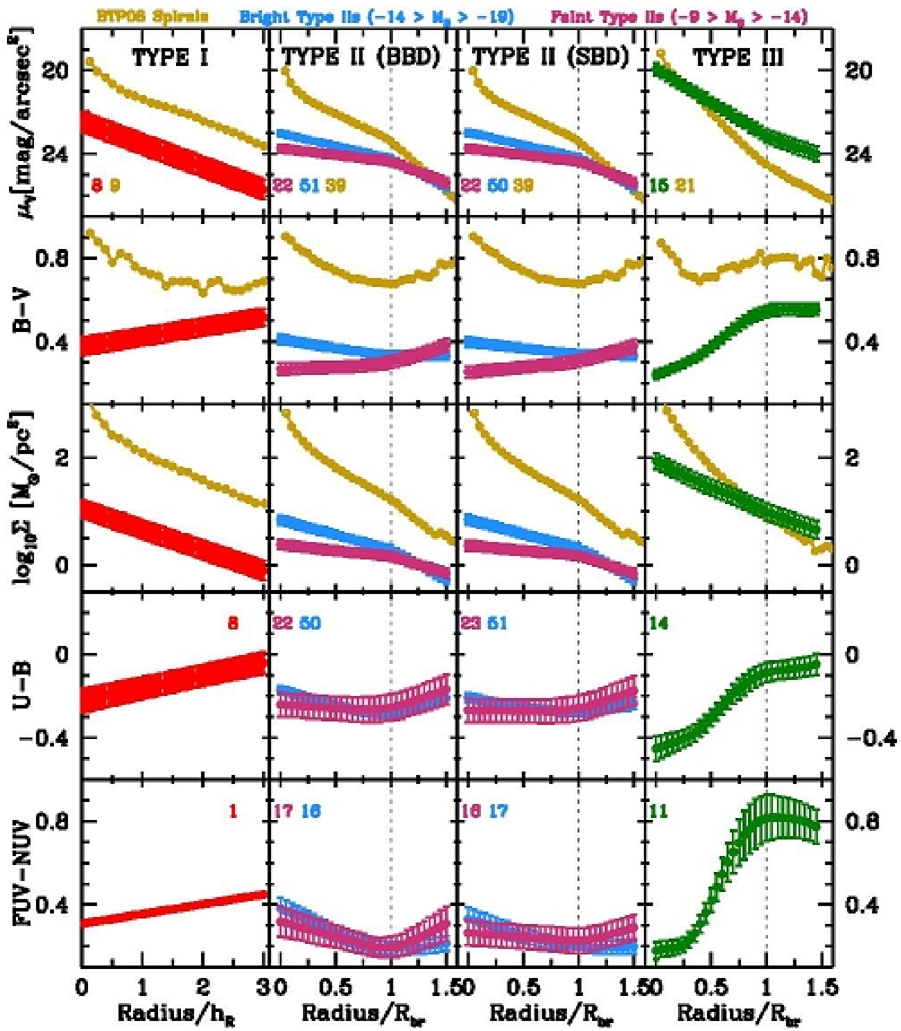

Astro-ph: 1606.01207

THE ISLANDS PROJECT II: THE LIFETIME STAR FORMATION HISTORIES OF SIX ANDROMEDA DSPHS

Evan D. Skillman[2], Matteo Monelli[3,4], Daniel R. Weisz[5,6], Sebastian L. Hidalgo[3,4], Antonio Aparicio[4,3], Edouard J. Bernard[7], Michael Boylan-Kolchin[8], Santi Cassisi[9], Andrew A. Cole[10], Andrew E. Dolphin[11], Henry C. Ferguson[12], Carme Gallart[3,4], Mike J. Irwin[13], Nicolas F. Martin[14,15], Clara E. Martínez-Vázquez[3,4], Lucio Mayer[16,17], Alan W. McConnachie[18], Kristen B. W. McQuinn[8], Julio F. Navarro[19], and Peter B. Stetson[18]

Draft version June 6, 2016

ABSTRACT

The Initial Star formation and Lifetimes of Andromeda Satellites (ISLAndS) project uses *Hubble Space Telescope* imaging to study a representative sample of six Andromeda dSph satellite companion galaxies. The main goal of the program is to determine whether the star formation histories (SFHs) of the Andromeda dSph satellites demonstrate significant statistical differences from those of the Milky Way, which may be attributable to the different properties of their local environments. Our observations reach the oldest main sequence turn-offs, allowing a time resolution at the oldest ages of ~ 1 Gyr, which is comparable to the best achievable resolution in the MW satellites. We find that the six dSphs present a variety of SFHs that are not strictly correlated with luminosity or present distance from M31. Specifically, we find a significant range in quenching times (τ_q, lookback times from 9 to 6

Позиции объектов на небе

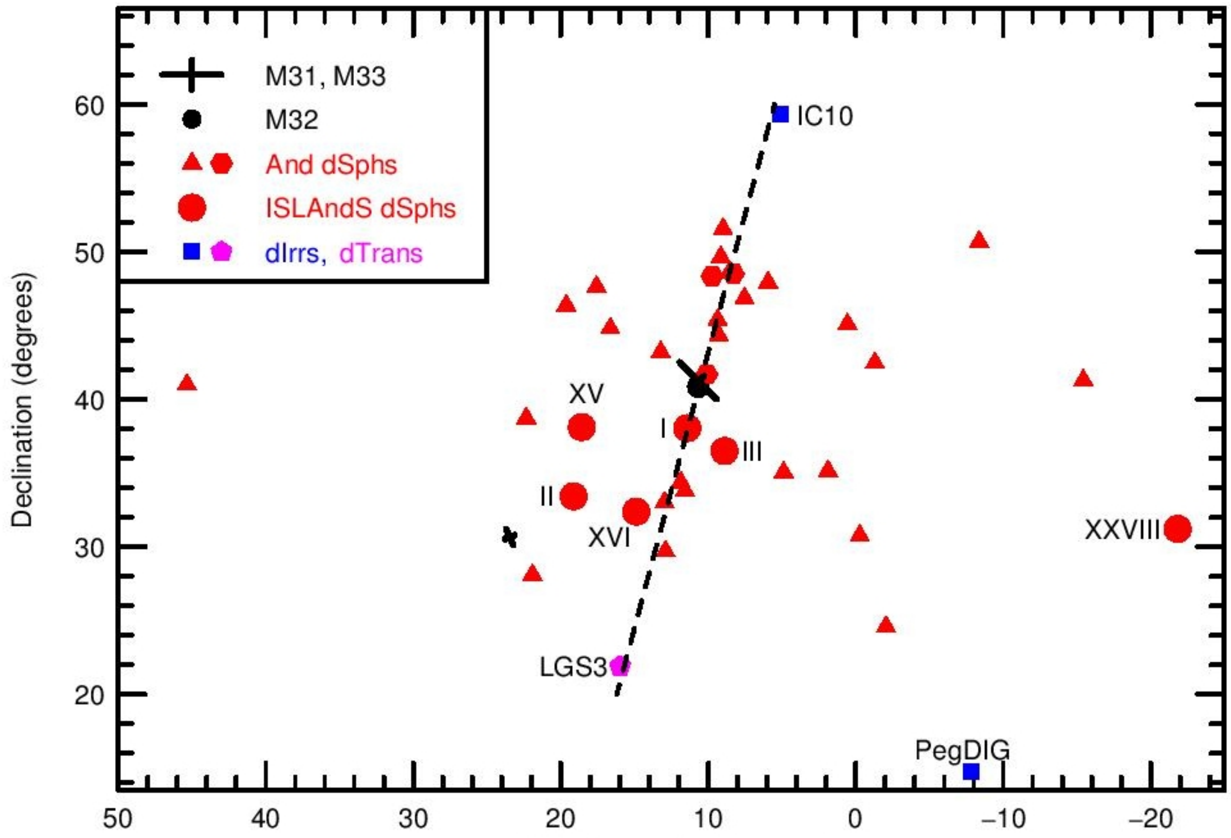

Свойства исследуемых спутников М 31

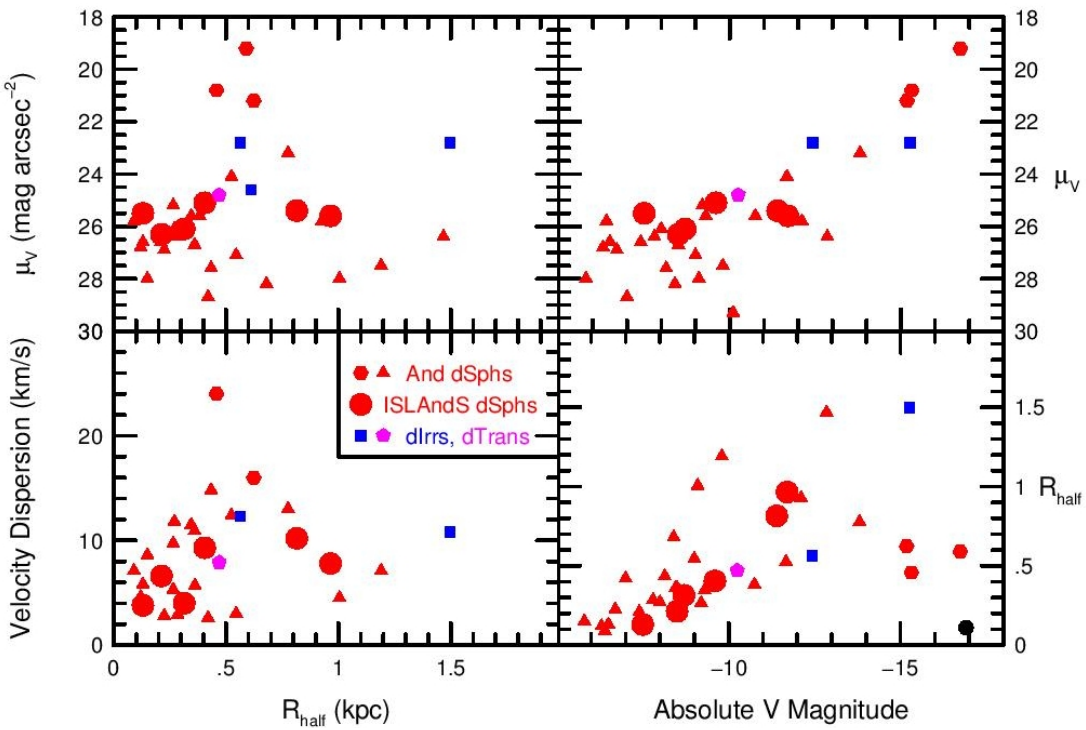

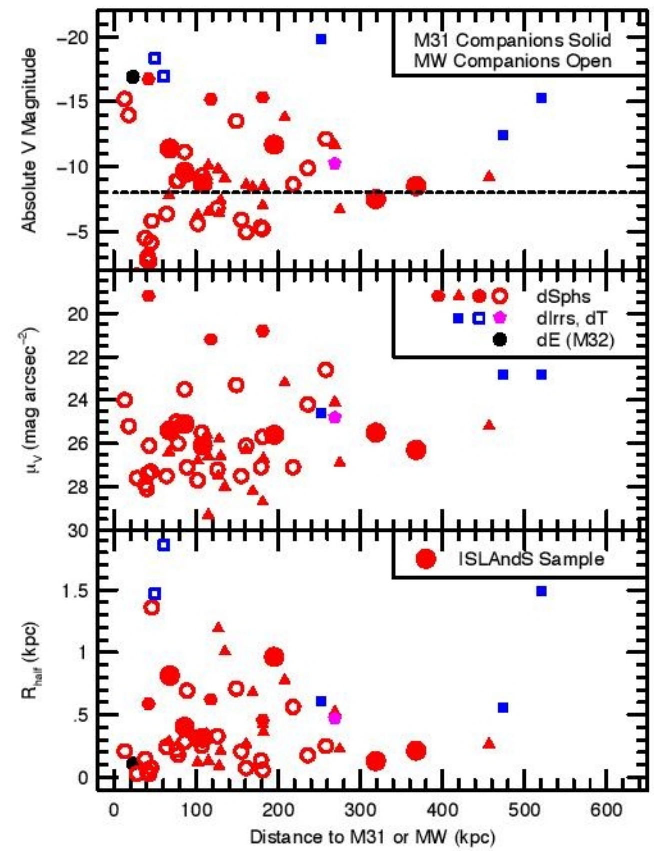

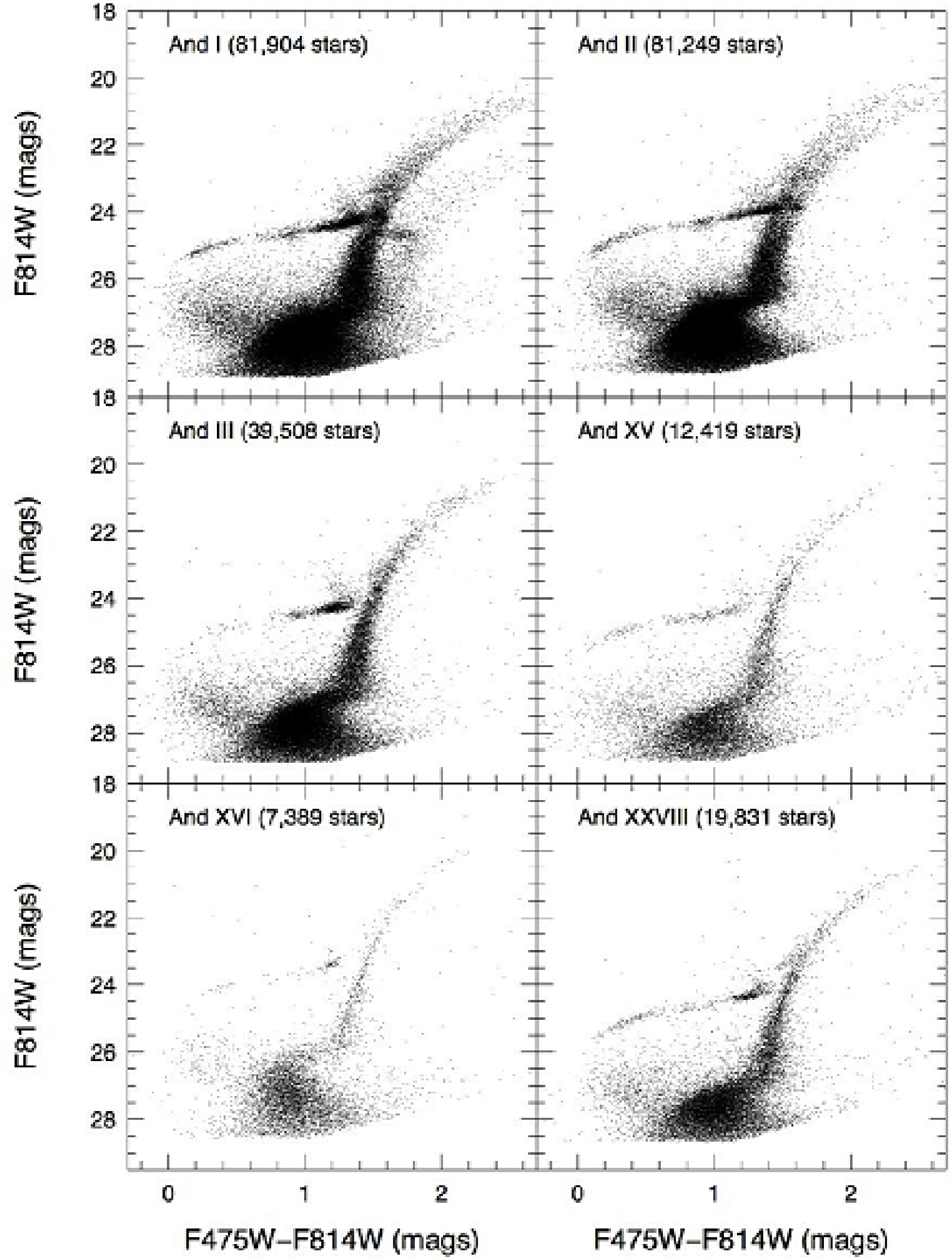
And I (81,904 stars)
And II (81,249 stars)
And III (39,508 stars)
And XV (12,419 stars)
And XVI (7,389 stars)
And XXVIII (19,831 stars)
F814W (mags)
F475W−F814W (mags)

Кумулятивная сборка

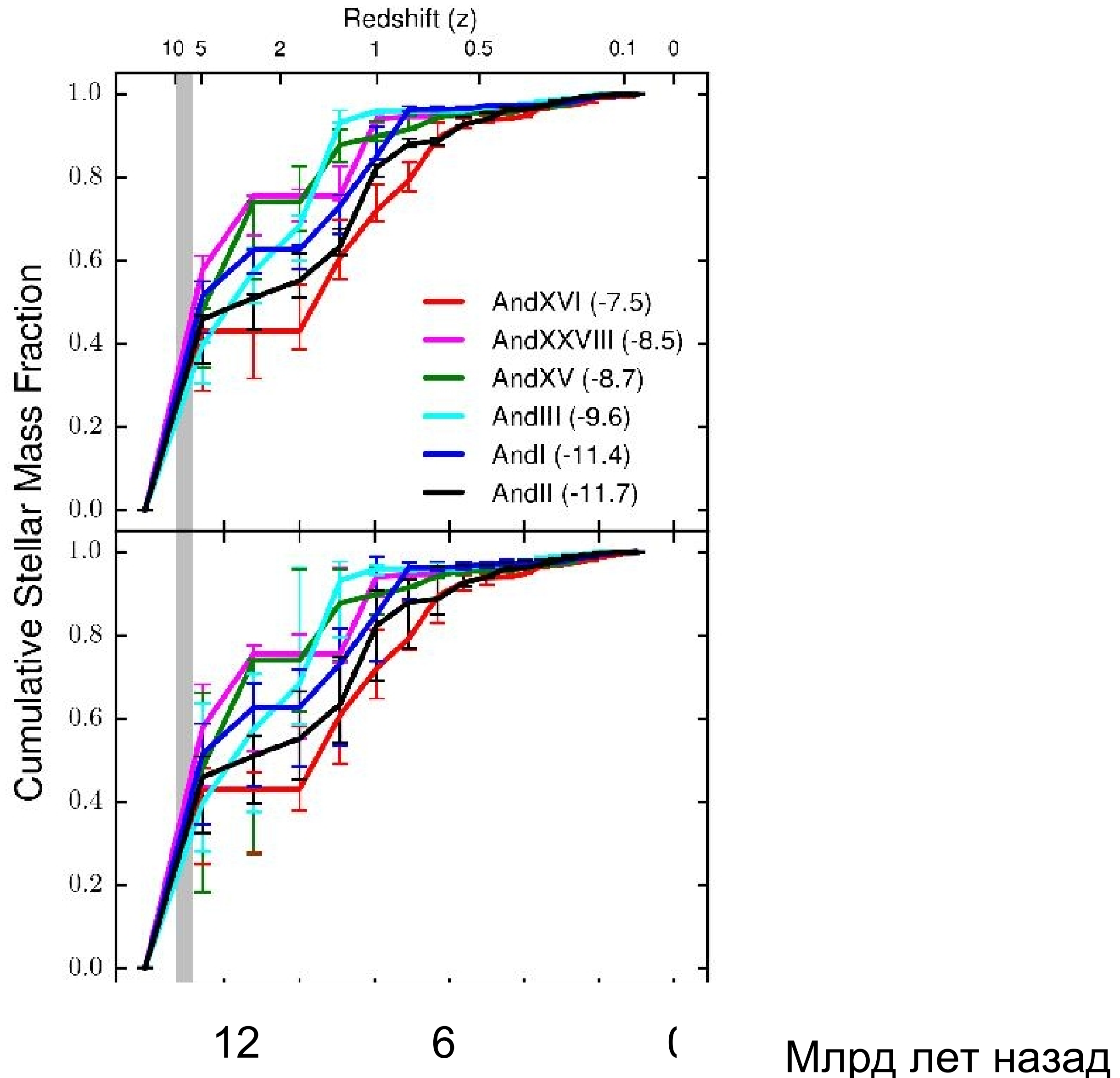

Сравнение со спутниками нашей Галалактики

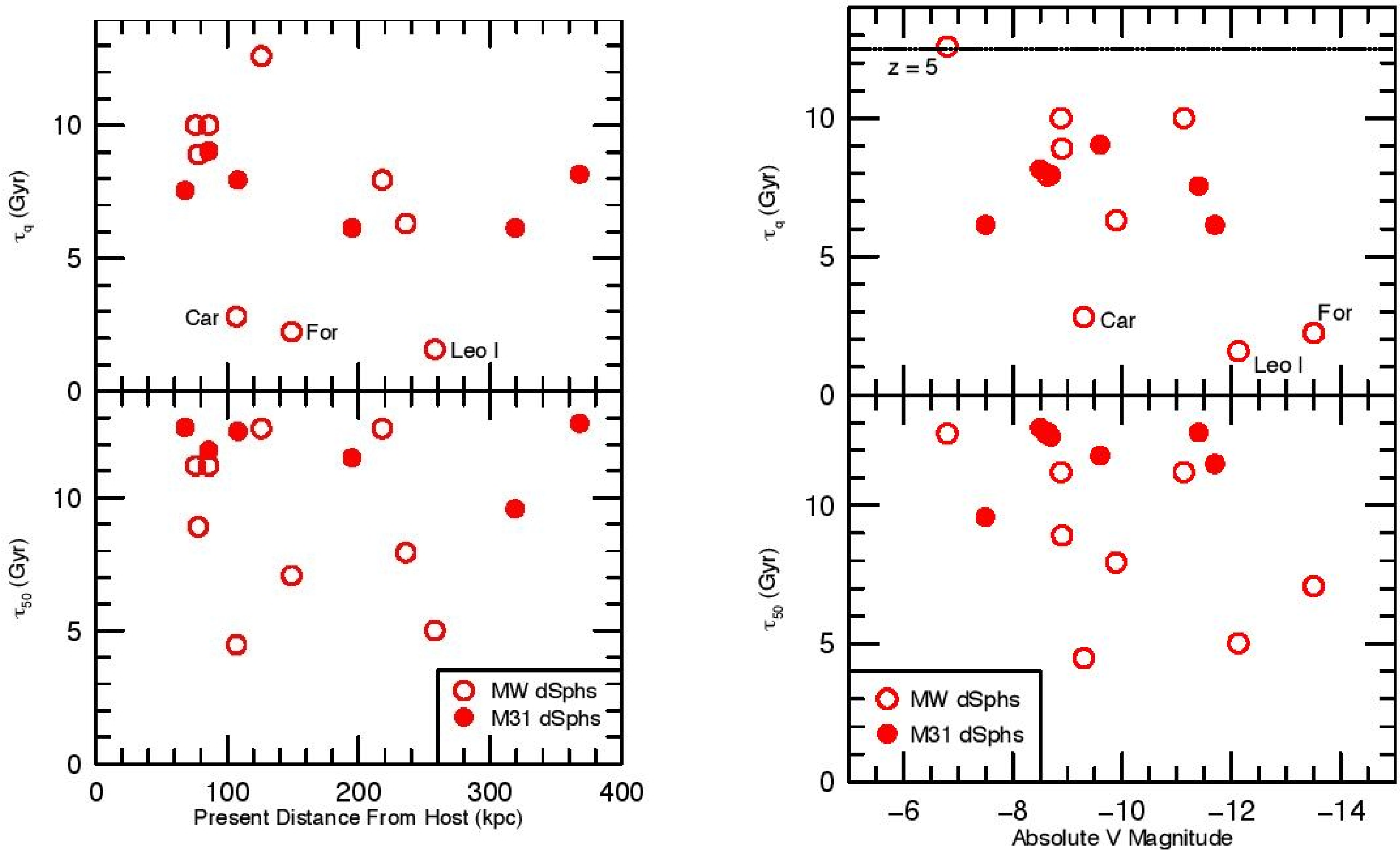

Была ли резкая остановка SF? И когда

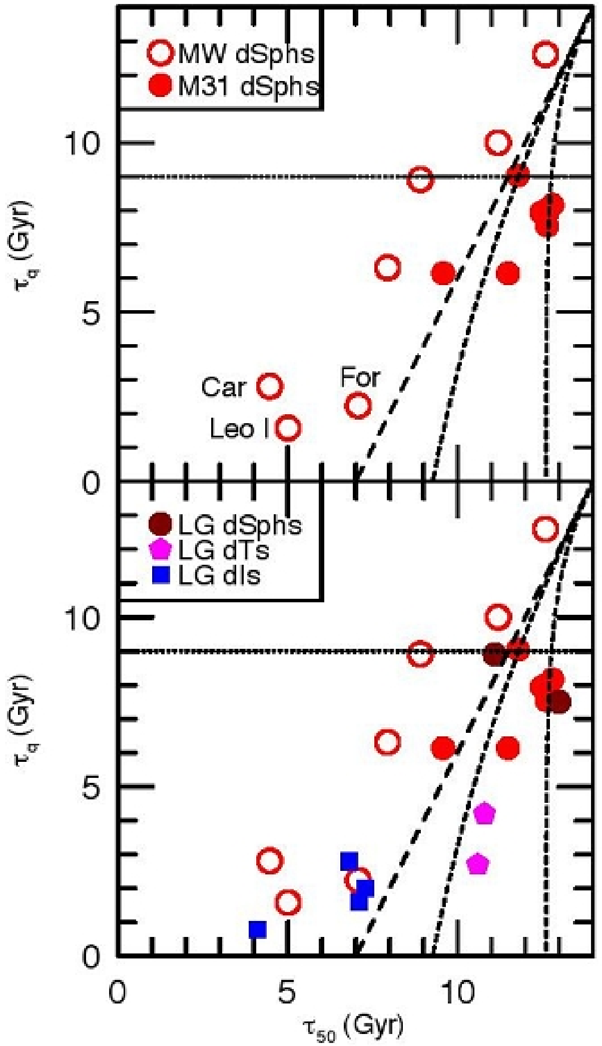

Astro-ph: 1606.01908

Variations of the initial mass function in semi-analytical models: implications for the chemical enrichment of galaxies in the GAEA model.

Fabio Fontanot[1⋆], Gabriella De Lucia[1], Michaela Hirschmann[2], Gustavo Bruzual[3], Stéphane Charlot[2] and Stefano Zibetti[4]

[1] *INAF - Astronomical Observatory of Trieste, via G.B. Tiepolo 11, I-34143 Trieste, Italy*
[2] *UPMC-CNRS, UMR7095, Institut d'Astrophysique de Paris, 75014, Paris, France*
[3] *Instituto de Radioastronomía y Astrofísica, UNAM, Campus Morelia, México*
[4] *INAF-Osservatorio Astrofisico di Arcetri, Largo Enrico Fermi 5, I-50125 Firenze, Italy*

Идеи Крупы

The IMF associated with individual stellar clusters is universal and can be well represented by a broken power law (Kroupa 2001):

$$\varphi_\star(m) = \begin{cases} \left(\frac{m}{m_{\rm low}}\right)^{-\alpha_1} & m_{\rm low} \leqslant m < m_0 \\ \left(\frac{m_0}{m_{\rm low}}\right)^{-\alpha_1}\left(\frac{m}{m_0}\right)^{-\alpha_2} & m_0 \leqslant m < m_1 \\ \left(\frac{m_0}{m_{\rm low}}\right)^{-\alpha_1}\left(\frac{m_1}{m_0}\right)^{-\alpha_2}\left(\frac{m}{m_1}\right)^{-\alpha_3} & m_1 \leqslant m \leqslant m_{\rm max} \end{cases}$$

where $m_{\rm low} = 0.1$, $m_0 = 0.5$, $m_1 = 1.0$, $\alpha_1 = 1.3$, $\alpha_2 = \alpha_3 = 2.35$. The shape of the IMF of individual clouds is usually

- IMF для звезд

over individual MCs, whose mass function is assumed to be a power-law

$$\varphi_{\rm CL}(M_{\rm cl}) \propto M_{rmcl}^{-\beta}, \quad (2)$$

- IMF для скоплений

Идеи Крупы

Weidner et al. (2004) using observed maximum star cluster masses (but it can be derived analytically also from optimal sampling arguments Kroupa et al. 2013):

$$\log M_{\rm cl}^{\rm max} = 0.746 \log SFR + 4.93 \qquad (3)$$

We limit[1] $M_{\rm cl}^{\rm max}$ to $2 \times 10^7 M_\odot$, and the mass of the smallest star cluster is set to $M_{\rm cl}^{\rm min} = 5 M_\odot$ corresponding to the individual groups in the Taurus-Auriga complex (Kroupa & Bouvier 2003).

At the same time, it is possible to numerically derive the most massive star (of mass $m_{\rm max}$) forming in a cluster, by imposing that it contains exactly one $m_{\rm max}$ star and using the universal IMF hypothesis. Pflamm-Altenburg et al. (2007) proposed the following fit to this numerical solution:

$$\log m_\star^{\rm max} = 2.56 \log M_{\rm cl} \times [\,3.82^{9.17} + (\log M_{\rm cl})^{9.17}\,]^{1/9.17} - 0.38 \qquad (4)$$

- Зависимость вернего предела масс от SF:
- Для скоплений

и для звезд

Модификации и подгонки

plain this result, Weidner et al. (2013) assumed that the β slope in Eq. 2 is not universal, but it also depends on SFR:

$$\beta = \begin{cases} 2 & SFR < 1 M_\odot/yr \\ -1.06 \log SFR + 2 & SFR \geqslant 1 M_\odot/yr \end{cases} \quad (5)$$

- Модификация IMF для скоплений

$$\alpha_3 = \begin{cases} 2.35 & \rho_{\rm cl} < 9.5 \times 10^4 M_\odot/pc^3 \\ 1.86 - 0.43 \log(\frac{\rho_{\rm cl}}{10^4}) & \rho_{\rm cl} \geqslant 9.5 \times 10^4 M_\odot/pc^3 \end{cases} \quad (6)$$

which, and has the advantage of being independent on metallicity. It is possible to theoretically derive the dependence of $\rho_{\rm cl}$ on $M_{\rm cl}$ (Marks & Kroupa 2012):

$$\log \rho_{\rm cl} = 0.61 \log M_{\rm cl} + 2.85 \quad (7)$$

- Модификация IMF для звезд

Чем отличается «интегральная по галактике» от начальной MF

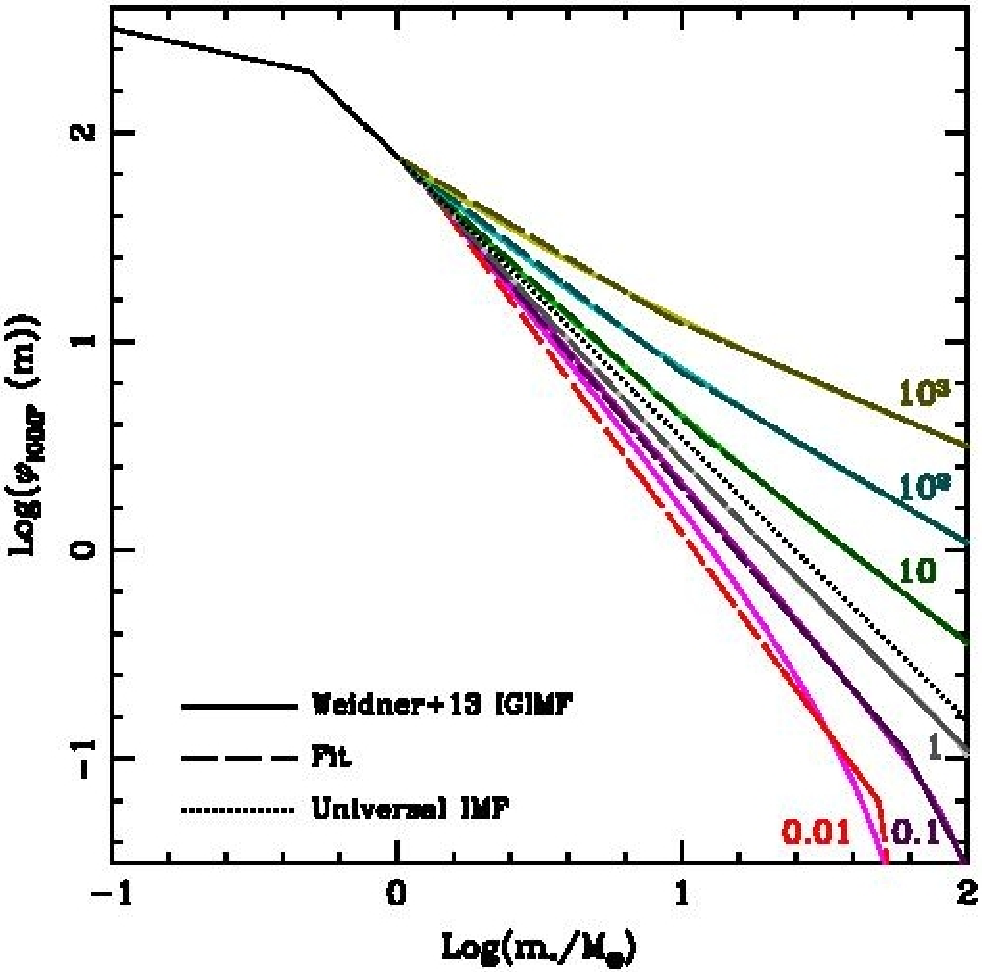

SF rate

Сравнение модели с данными z=0

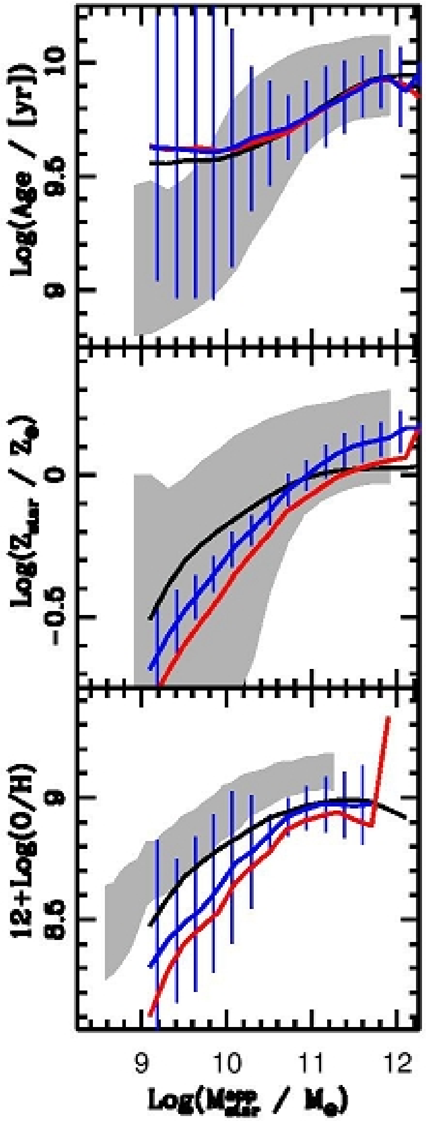

Table 2. Parameter values adopted for the runs considered in this study.

Parameter	HDLF16	High-α_{SF} model	Low-α_{SF} model
α_{SF}	0.03	0.19	0.1
ϵ_{reheat}	0.3	0.575	0.885
ϵ_{eject}	0.1	0.12	0.06
γ_{reinc}	1.0	1.0	0.68
$\kappa_{radio}/10^{-5}$	1.0	1.78	0.87

Сравнение модели с данными z=0-3

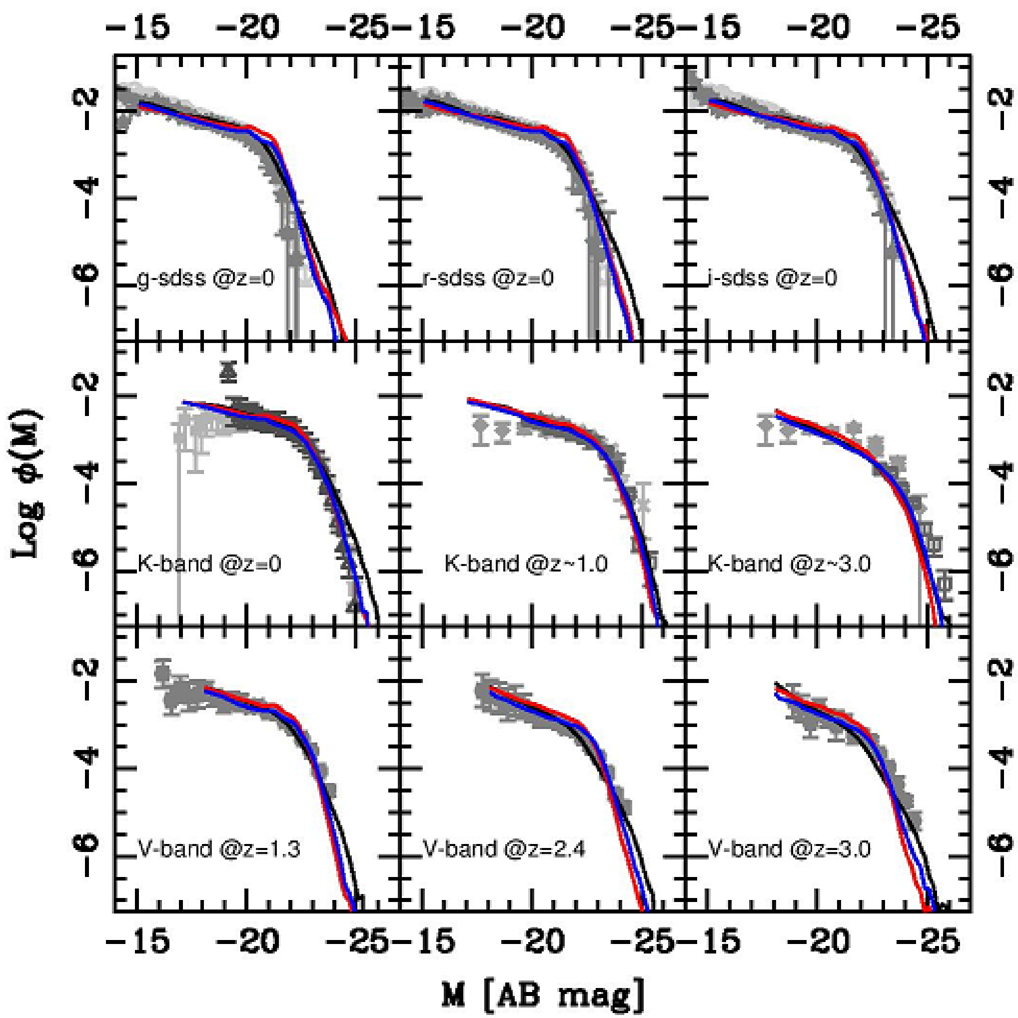

Основной успех!

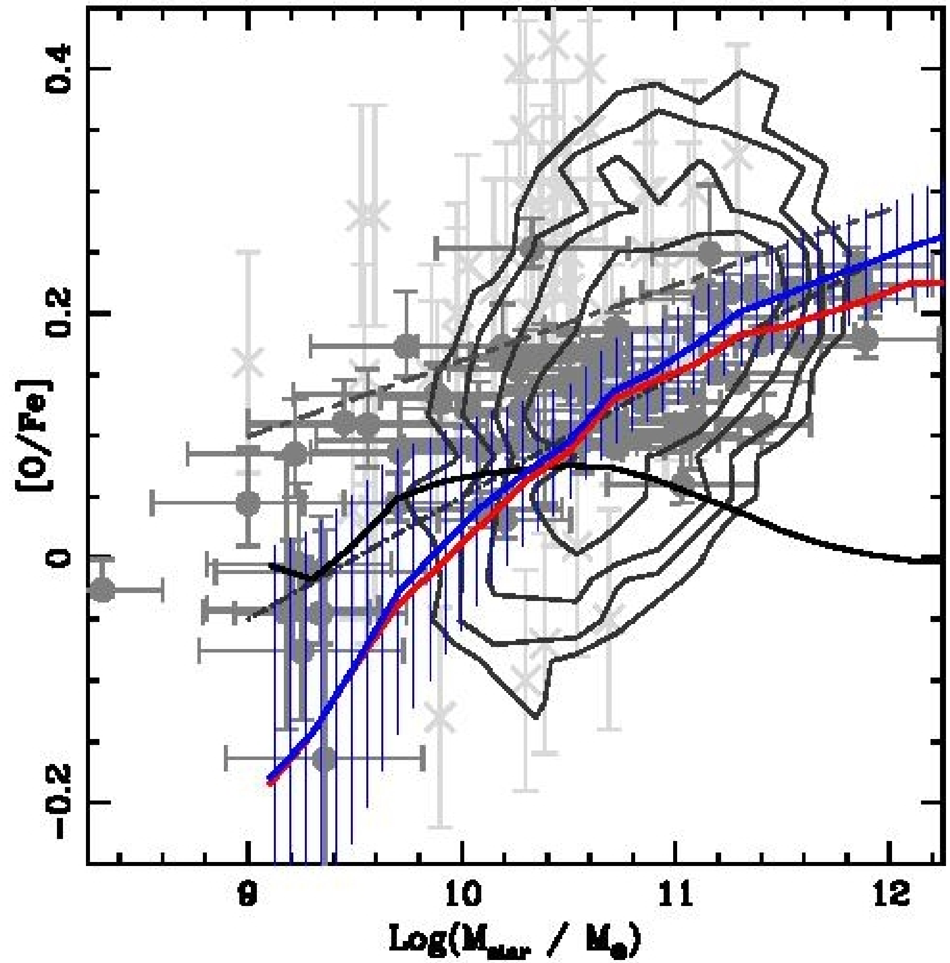

Figure 5. [O/Fe] ratios as predicted by GAEA compared to observed [α/Fe] ratios for local elliptical galaxies. Lines, colours and hatched area are as in Fig. 3 (only model galaxies with $B/T > 0.7$ have been in-

Переход к «интегральной по галактике» IMF сильно поправляет прогноз

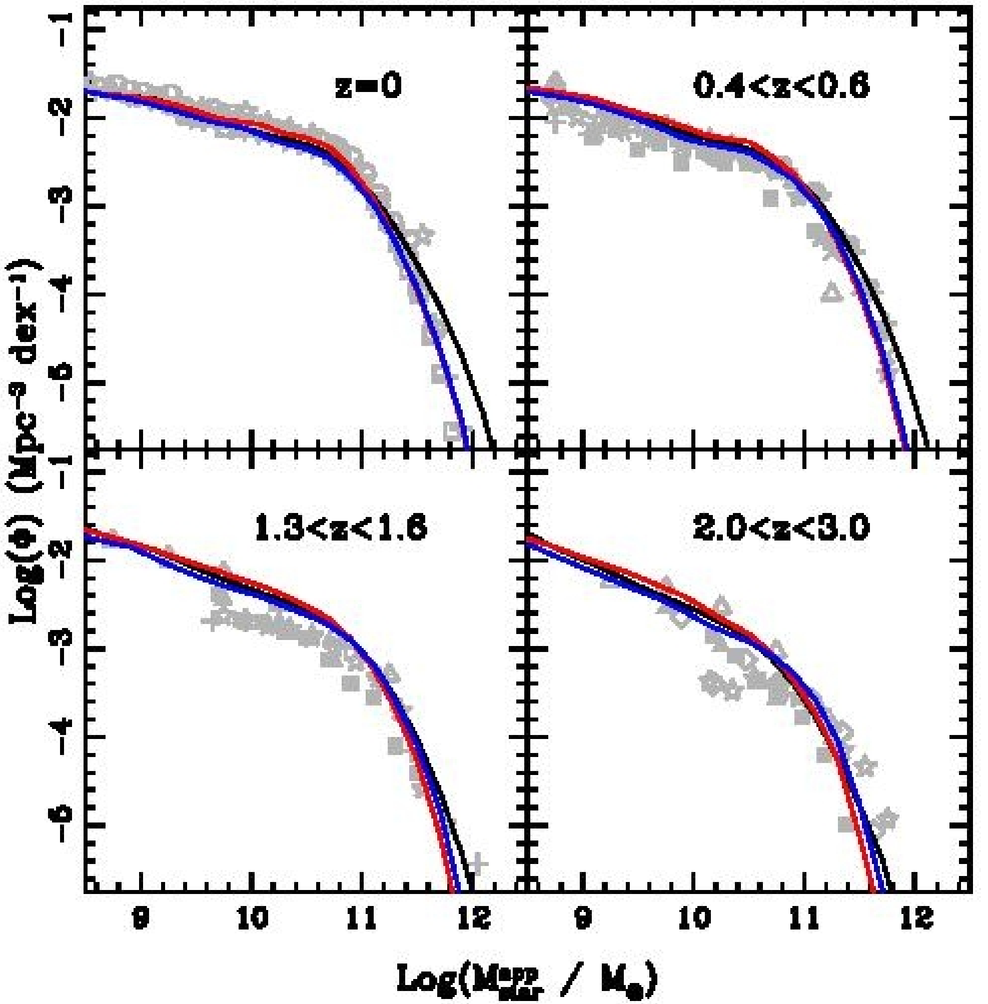

Истории формирования

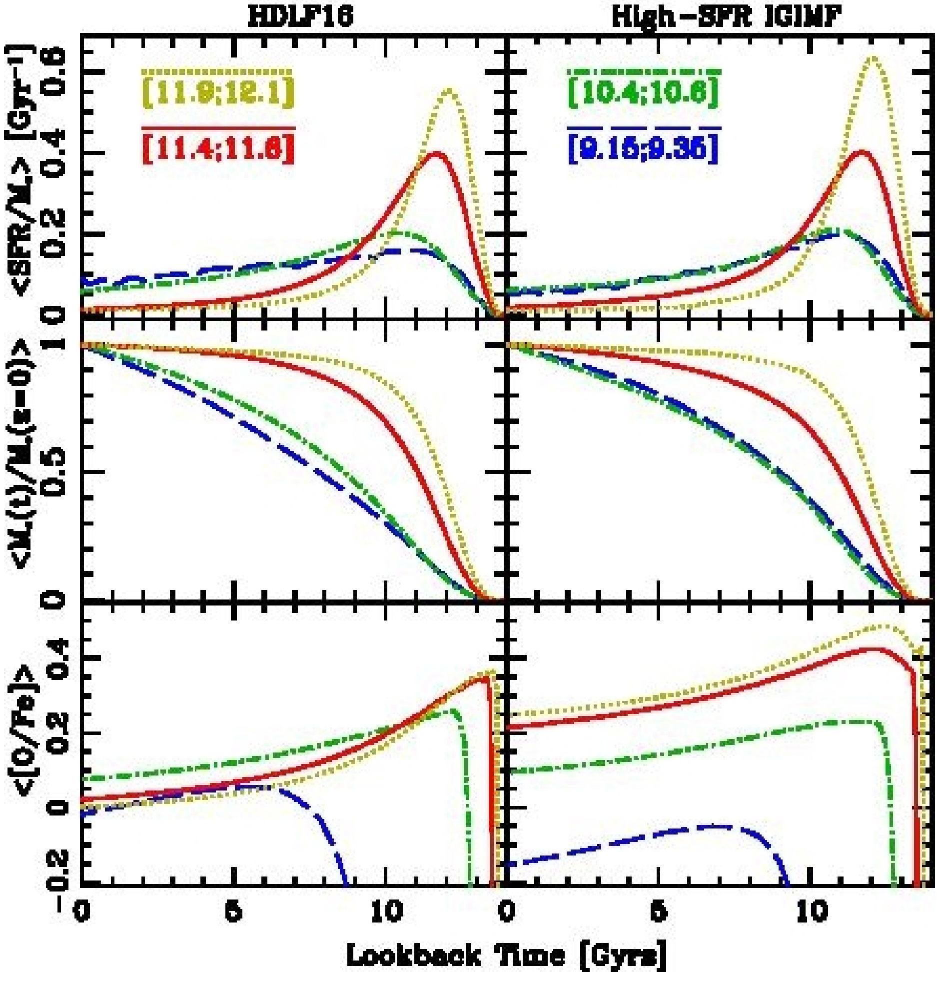

Figure 8. Mean evolutionary histories for galaxies in different $Log(M/M_{\odot})$ intervals (as indicate in the caption) in the HDLF16 (left column) and High-$\alpha_{\rm SF}$ (right column) runs. *Upper panels*: mean normalised